Pictorial Essay

J Korean Soc Radiol 2020;81(2):351-364
https://doi.org/10.3348/jksr.2020.81.2.351
pISSN 1738-2637 / eISSN 2288-2928

대한영상의학회지

Missed Lung Cancers on Chest Radiograph: An Illustrative Review of Common Blind Spots on Chest Radiograph with Emphasis on Various Radiologic Presentations of Lung Cancers

놓치기 쉬운 폐암: 흉부 X선 진단의 함정에 대한 이해와 다양한 폐암 영상 소견의 중요성

Goun Choi, MD[1], Bo Da Nam, MD[1], Jung Hwa Hwang, MD[1]*, Ki-Up Kim, MD[2], Hyun Jo Kim, MD[3], Dong Won Kim, MD[4]

Departments of [1]Radiology, [2]Respiratory and Allergy Medicine, [3]Cardiothoracic Surgery, [4]Pathology, Soonchunhyang University Hospital, Seoul, Korea

Missed lung cancers on chest radiograph (CXR) may delay the diagnosis and affect the prognosis. CXR is the primary imaging modality to evaluate the lungs and mediastinum in daily practice. The purpose of this article is to review chest radiographs for common blind spots and highlight the importance of various radiologic presentations in primary lung cancer to avoid significant diagnostic errors on CXR.

Index terms Lung Neoplasms; Lung; Radiography; Tomography, X-Ray Computed

Received July 5, 2019
Revised August 14, 2019
Accepted August 24, 2019

***Corresponding author**
Jung Hwa Hwang, MD
Department of Radiology, Soonchunhyang University Hospital, 59 Daesagwan-ro, Yongsan-gu, Seoul 04401, Korea.

Tel 82-2-709-9396
Fax 82-2-709-9066
E-mail jhhwang@schmc.ac.kr

ORCID iDs
Goun Choi
https://orcid.org/0000-0003-4303-4764
Bo Da Nam
https://orcid.org/0000-0001-7822-6104
Jung Hwa Hwang
https://orcid.org/0000-0003-4426-3673
Ki-Up Kim
https://orcid.org/0000-0002-9736-7356
Hyun Jo Kim
https://orcid.org/0000-0003-0820-1782
Dong Won Kim
https://orcid.org/0000-0003-0154-124X

INTRODUCTION

A chest radiograph (CXR) remains as an important primary imaging modality for evaluating the lungs and mediastinum in daily practice and provides vast quantities of use-

ful information (1). A CXR is a two-dimensional presentation of a three-dimensional structure which includes many overlapping structures (2). The information derived from the configurations and interrelationships of anatomic structures in the lung, mediastinum, and pleura forms the basis of the "lines and stripes" concept, and it plays a valuable role in establishing a diagnosis (1).

The generally accepted error rate for the radiologic diagnosis of early lung cancer is between 20% and 50% (3). A missed lung cancer on CXR may delay diagnosis and affect the patient's prognosis (3-6). The significantly higher median length of time from the first positive radiograph to the time of starting treatment was found in patients with overlooked lesions than in those without preceding abnormalities (4). In the study by Kashiwabara et al. (6), the outcome in stage I–II patients with missed tumors measuring over 20 mm was worse than those with 20 mm or less.

The major contributing factors of missed lung cancer on CXR are superimposed normal structures (3). The factors contributing to missed lung cancer on CXR can be classified as an observer error, tumor characteristics, and technical considerations (5). An observer error is likely the largest cause of misdiagnosis of lung cancer on a CXR. The causes of an observer error can be further classified into three categories: visual scanning error, recognition error, and decision-making error. The most important consideration of tumor characteristics is dimension, conspicuity, and location. Image quality, patient positioning, and movement are important technical determinants of the probability of overlooking pulmonary abnormality (4, 5).

An observer error can be reduced by optimizing the perception and enhancing the radiologic interpretation of the radiologists in chest reading methodology and in chest diseases through training (5). Familiarity with common blind spots on CXR and strategies for evaluating difficult areas can help to avoid missing significant findings. To further enhance radiologic interpretation, radiologists should be aware of various presentations of lung cancer (7). Recently, advances in deep learning techniques demonstrated promising results in medical imaging tasks including pulmonary nodule detection and diagnosis of tuberculosis (8, 9), which showed high performance in the classification of normal and abnormal findings on CXR (10). Nevertheless the recent technical advancement, still the role of every radiologist by extending their fundamental knowledge and enhancing expertise in image interpretation need to be emphasized. The purpose of this article is to review with illustrations, address the importance of radiologic common blind spots, and to highlight the criticality of knowing various radiologic presentations of primary lung cancer to avoid significant diagnostic errors on CXR.

REVIEW OF RADIOLOGIC COMMON BLIND SPOTS

APICAL LUNG ZONES

The predominance of overlooked pulmonary tumors in the apical zones was reported to be 72% in the study of Shah et al. (11), in which missed lung cancers were mainly located in the apical or posterior segment (60%). The location contains little lung parenchyma compared to overlying soft tissue and bone. Anterior 1st rib and posterior 3rd to 4th ribs make lung apices to be overall increased opacity (Fig. 1). There could be often asymmetric calcification of the first costal cartilage. Thickening of extrapleural fat, dense pleural and subpleural fibrosis could

Fig. 1. A 67-year-old man with a squamous cell carcinoma.
A. A subtly increased opacity is retrospectively identified in the apex of the right lung overlapping with the bony thorax (arrow), which was overlooked on the initial CXR. Right pleural thickening is also seen with obliteration of the costophrenic sulcus.
B, C. A year later, the tumor is enlarged with direct chest wall invasion and rib destruction, as seen on follow-up CXR and CT.
CXR = chest radiograph

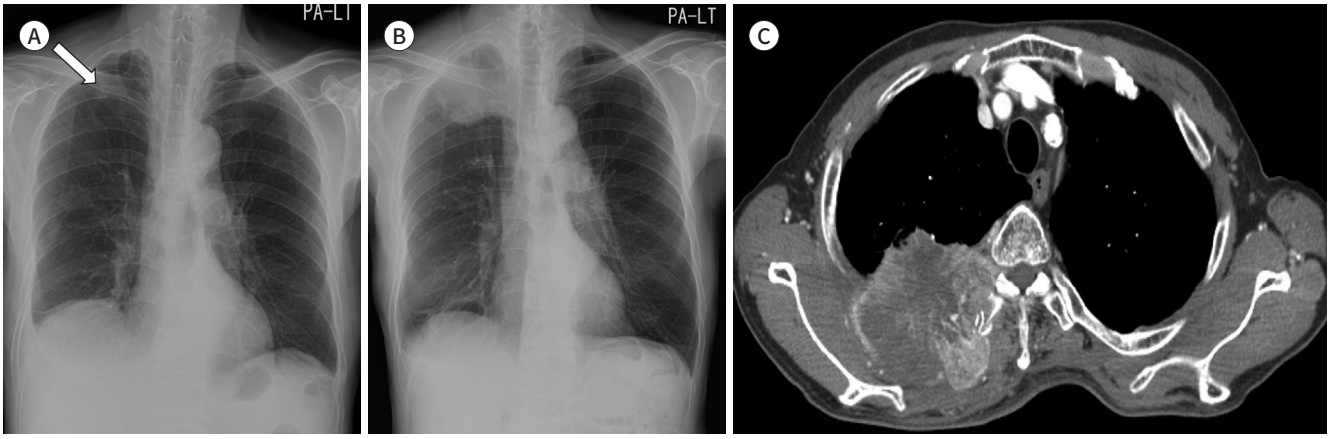

be presented as thickening of apical pleural caps, usually less than 5 mm in thickness, which is not unusual finding with no clinical significance (2, 12). When a CXR reveals asymmetry of the pulmonary apices, irregular pleural thickening more than 5 mm or bone destruction, a malignancy such as Pancoast tumor should be suspected (13).

PARAMEDIASTINAL REGION

A paramediastinal region is the second most common location of missed lung cancer. Mediastinum is a relatively small space, which is full of vital structures, and the mediastinal stripe is often overlapped with normal mediastinal anatomy. Therefore, familiarity with the normal contours and lines of the mediastinum is important to detect subtle abnormalities (14, 15). Careful assessment of normal anatomic lines, stripes, and interfaces is essential for accurate radiologic interpretation. Normal mediastinal lines on CXR include anterior and posterior junction lines. Stripes are thicker lines formed by air outlining thicker intervening soft tissue, including left and right paratracheal stripes (Fig. 2) and posterior tracheal stripe. Interfaces are formed when structures of different densities come in contact with one another. Many interfaces are seen on a CXR, including right and left paraspinal interfaces, azygoesophageal recess and aortopulmonary window (Fig. 3), which are important in the radiologic evaluation of mediastinal diseases (1).

The assessment of central tracheobronchial trees is also important. The air-filled trachea is usually distinct as a tubular lucency extending inferiorly from the thoracic inlet. The anterior tracheal wall is approximately 1–2 mm in thickness and the posterior tracheal stripe (tracheoesophageal stripe) can range 2–6 mm in thickness depending on esophageal distention (1).

PULMONARY HILA

A pulmonary hilar region is the most difficult part of radiologic interpretation on a CXR and is a common location of missed lung cancers. Muhm et al. (16) reported 65% of the missed cancers locating at the pulmonary hilum. Anatomically, hila are composed of many important an-

Fig. 2. A 55-year-old man with a small-cell lung cancer.
A. On initial chest radiograph, obliteration of the right paratracheal stripe (arrowheads) can be identified with a slightly increased paratracheal opacity.
B. Approximately 3 months later, the tumor is enlarged with obliteration of the right and left paratracheal stripes (arrowheads), which is associated with mediastinal widening and contour bulging. On contrast-enhanced CT, right central lung cancer with conglomerated bilateral mediastinal lymphadenopathy is noted.

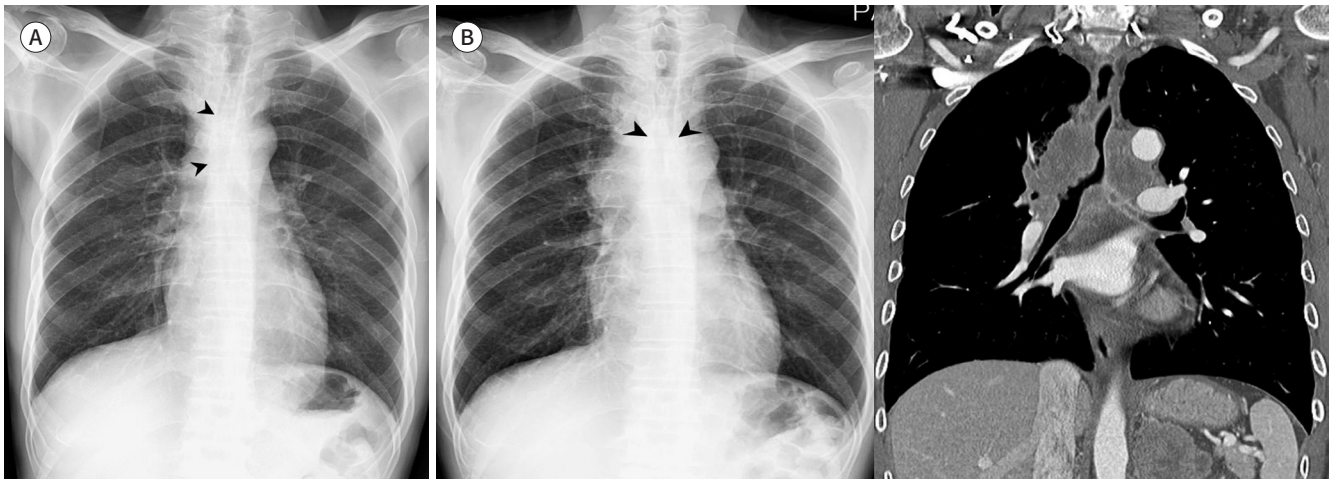

Fig. 3. A 77-year-old man with a squamous cell carcinoma.
A. Subtly increased opacities in the left hilar and perihilar areas (arrow) are retrospectively identified on the initial CXR. Mild bilateral pleural thickening with right pleural calcifications are also seen.
B. Approximately 4 months later, contour bulging and lateral convexity at the aortopulmonary window (arrows) and left hilum are noted on CXR. The mild left hemidiaphragmatic elevation is because of tumor invasion of the left phrenic nerve. A heterogeneously enhanced lobulated mass is noted at the center of the left upper lobe, which shows direct mediastinal invasion at the aortopulmonary window (arrowheads) on CT.
CXR = chest radiograph

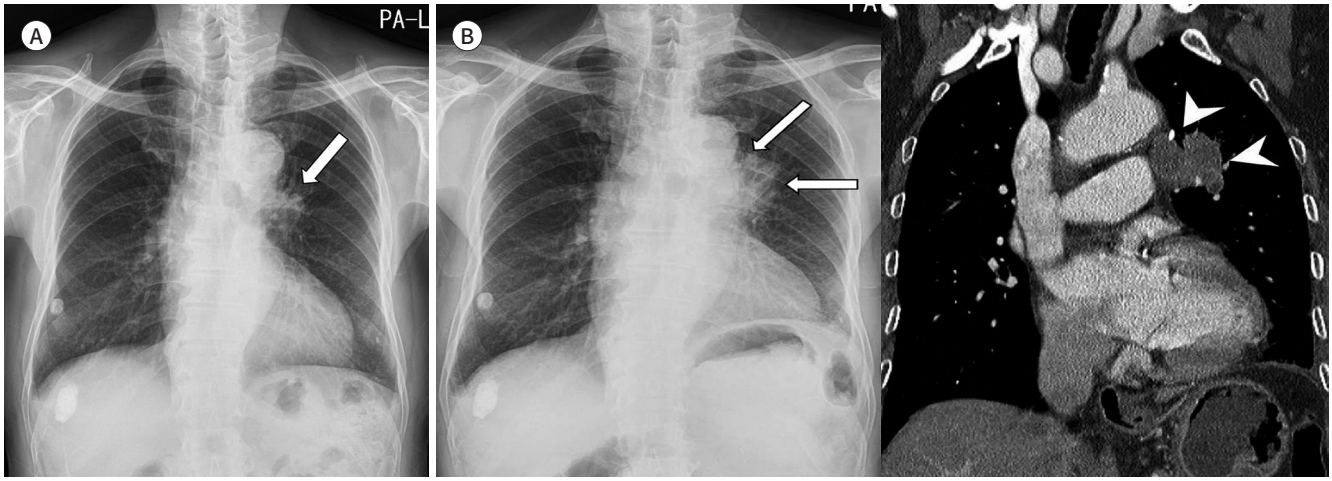

atomical structures including pulmonary vessels, major bronchi, and lymph nodes. A wide variety in the appearance of a normal hilum makes it difficult to judge whether the seen abnormality is true or not. Initial assessment for hilar abnormality on a frontal CXR is to find the normal concave angle of pulmonary hilum, which is formed superiorly by superior pulmonary veins and inferiorly by interlobar pulmonary arteries. The position of hila is also important and left hilum is usually located slightly higher than the right hilum. Review of the correlation with

Fig. 4. A 70-year-old woman with a squamous cell carcinoma.
A. On the initial chest radiograph, mild bilateral hilar asymmetry with slightly dense right hilum is retrospectively identified in the frontal view (arrow).
B. Approximately 3 months later, the right hilar mass shows enlargement with lateral contour bulging and is well-delineated in both frontal and lateral views with obliteration of the inferior hilar window (arrowheads) in the lateral view.

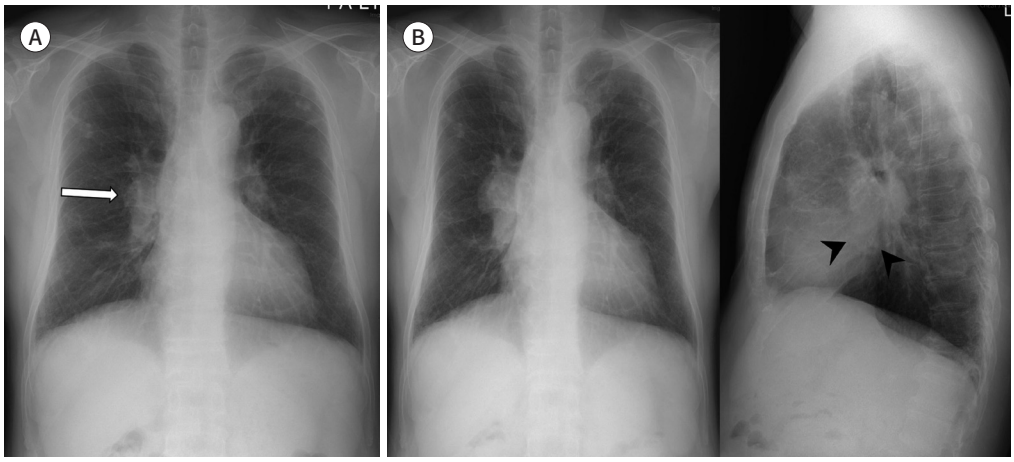

Fig. 5. A 75-year-old man with a squamous cell carcinoma.
A. A mass is seen at the right hilum, and branches of the right pulmonary artery converge toward the relatively medially located right pulmonary artery (arrows) rather than a bulging right hilar mass (asterisk) ("hilum convergence sign") on chest radiograph and CT. Furthermore, the normal pulmonary vessels are in contact with the right hilar mass and the lateral silhouette of the vessels is partly obliterated ("hilum overlay sign").
B. The mass is seen in the hilar area with obliteration of the inferior hilar window (arrowhead) in the lateral view.

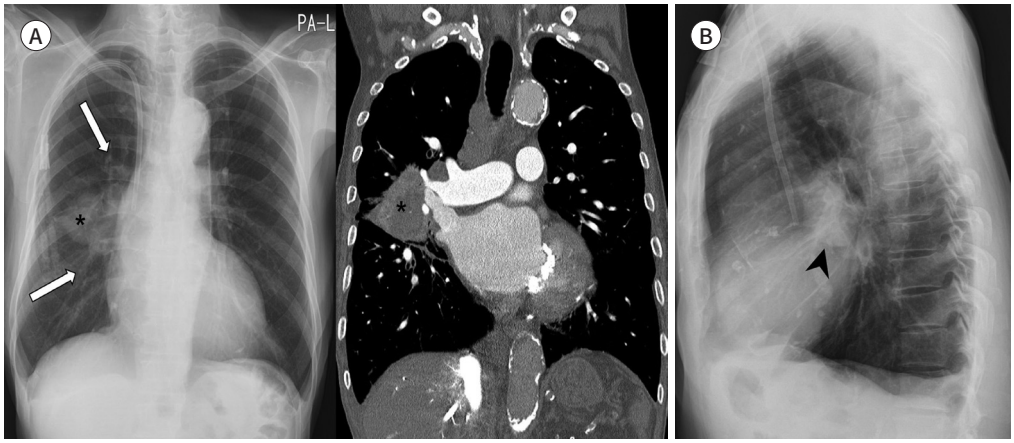

the lateral radiograph is beneficial to identify abnormalities in the hila, inferior hilar window (Figs. 4, 5), and the lungs posterior to the hila. There are no definite measurement criteria for hilar enlargement but hilar asymmetry always should not be ignored (Fig. 4) (17, 18).

There are four criteria for assessing pulmonary hilum: shape (S); a branching vascular appearance is normal, opacity (O); gradually diminishes toward the periphery, absolute size (A); not reliable unless enlargement is considerable, compare left and right for symmetry, proportionate size (P) ("SOAP"); two-thirds of the vascular density is in the lower portion of hila (18). There are few radiological signs that are helpful in assessing hilum. "Hilum convergence sign" is a useful chest radiographic sign to help distinguish a bulky hilum due to pulmonary artery

Fig. 6. A 62-year-old woman with an adenocarcinoma.
A. An obscure round mass is seen in the left retrocardiac region (arrow), which can easily be missed on the initial chest radiograph.
B. Approximately 2 years later, the mass is found to be enlarged in the left lower lobe in frontal and lateral views (arrows).

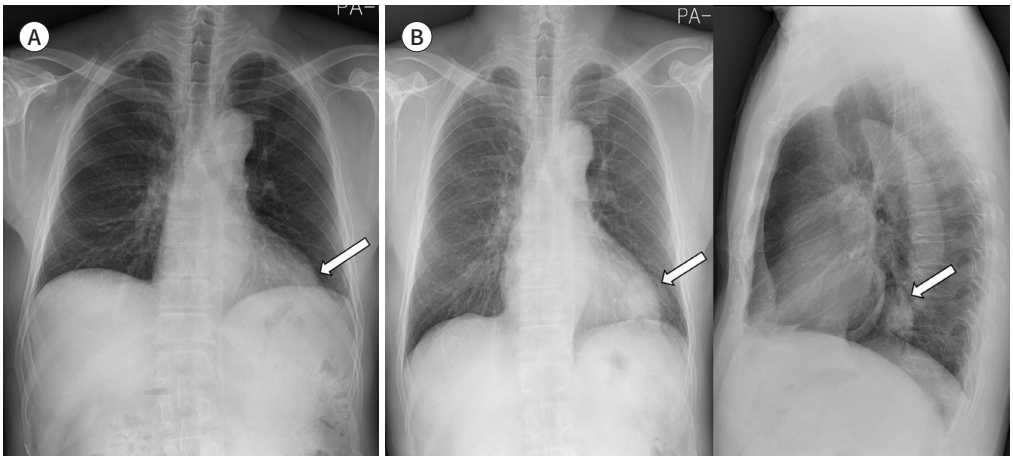

dilatation from a hilar mass (Fig. 5). Pulmonary vessels can be seen to invariably converge and join a dilated central pulmonary artery. "Hilum overlay sign" is silhouette sign of the hilum. If hilar vessels can be clearly seen over the lesion, the lesion is anatomically located anterior or posterior to the hilum. Instead, if hilar vessels cannot be well discriminated from the lesion, the lesion is located at the hilum (Fig. 5). It can also be thought of in another way. If the hilar pulmonary arteries are visible, more than a centimeter within the lateral edge of the mediastinal silhouette, then the lesion is not a cardiac silhouette. Most of these masses are found to be in the anterior mediastinum and hilum overlay sign is useful in differentiating cardiac enlargement from a mediastinal mass (18).

RETROCARDIAC REGION AND PARAVERTEBRAL REGIONS

On chest posterior-anterior (PA) view, the cardiac shadow may obscure the conspicuity of the paravertebral regions and retrocardiac lower lobes. More parts of the left lower lobe are obscured by the cardiac shadow than the right lower lobe. Windowing the radiograph to increase the visibility of the retrocardiac structures and "seeing through" is essential for recognition of pathology in this region (Fig. 6) (15, 17).

A lateral radiograph is often helpful for evaluation of abnormality in retrocardiac lower lobe when it shows "spine sign," which is an interruption in the progressive increase in lucency as one looks down the thoracic vertebral bodies from the neck to the diaphragms (19).

EXTRAPULMONIC PATHOLOGY

A serious extrapulmonic pathology can be an initial manifestation on a CXR. Even the subphrenic basal lungs, the posterior and lateral basal segments of both lower lobes are difficult to well evaluate on a chest PA view. Lung bases are one of the radiologic common blind spots (15) because which are overlapped with the abdominal organs covered by the diaphragms (Fig. 7A).

A careful assessment of the upper abdomen, soft tissues and bones will help to avoid miss-

Fig. 7. Extrapulmonary pathologies on chest radiograph.
A. A 68-year-old man with an adenocarcinoma shows a mass opacity in the basal segment of the right lower lobe (arrowheads) overlapping with the right hemidiaphragm and hepatic shadow in the posteroanterior view. Reticular opacities in the periphery of both the lower lobes suggest interstitial pulmonary fibrosis. Axial chest CT shows peripheral lung cancer in the right lower lobe (arrow).
B. A 37-year-old man shows a retrocardiac paraspinal bulging opacity (arrows) with obliteration of the azygoesophageal recess (arrowheads), which is a malignant esophageal submucosal tumor.
C. An 82-year-old man with prostate cancer shows extensive osteolytic and osteosclerotic bone metastases in the entire axial skeleton.

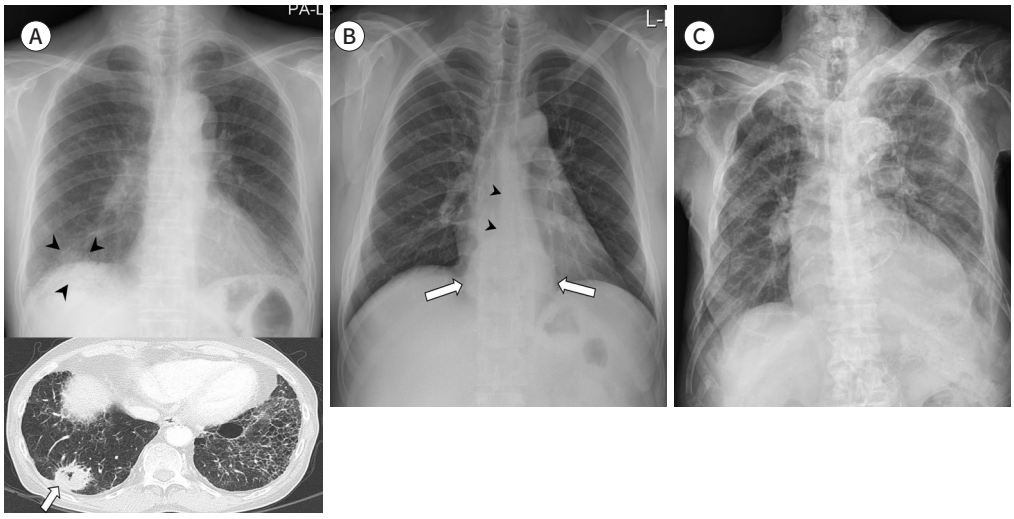

ing important ancillary findings (Fig. 7B). The upper abdomen is partly included in most of the chest radiographs. Windowing to increase the abdominal transparency may be helpful for evaluation of free intraperitoneal air and other significant intra-abdominal pathologies (17, 20). Abnormalities in the subcutaneous tissue, musculature and bony thorax of the chest wall (Fig. 7C), those of peripheral parts of the chest, can be easily overlooked in daily practice.

VARIOUS RADIOLOGIC PRESENTATIONS OF LUNG CANCER

CALCIFICATIONS

The presence of calcium within pulmonary lesions on radiologic examinations is an important finding for lesion characterization. For example, dense central, laminar, popcorn or diffuse calcifications establish a benign nature of pulmonary nodules (21). On the other hand, the presence of calcification in the solitary pulmonary nodule or mass does not always represent benignancy (7, 22). The widespread use of CT increased the sensitivity of detecting calcification in malignant tumors (21, 23). However, radiological demonstration of calcification in lung cancers is not common and can lead to misdiagnosis. In a malignant pulmonary nodule, calcification appears in the larger lesions and is usually stippled or eccentric. Amorphous, punctate and reticular patterns of calcification have been described in lung cancer (Fig. 8) (21). Also, malignant tumors may engulf a pre-existing calcified granuloma and tumor necrosis can lead to dystrophic calcifications. Particularly in mucinous adenocarcinoma, calcification may occur as a primary phenomenon (Fig. 8) (21).

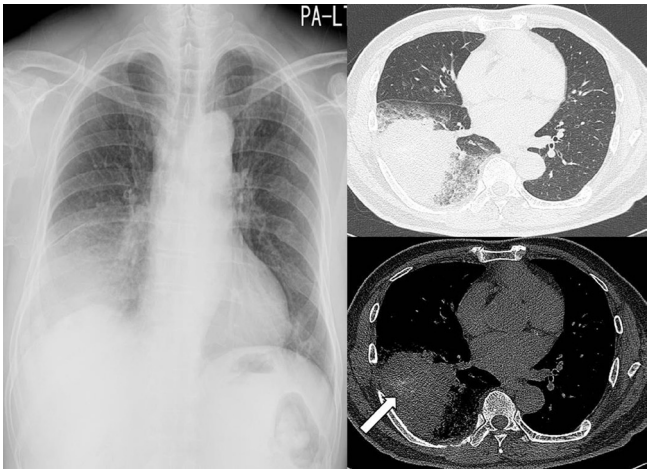

Fig. 8. A 65-year-old man with an invasive mucinous adenocarcinoma. A segmental air-space consolidation with a peripheral ground-glass opacity is noted in the right lower lobe on chest radiograph and CT, mimicking pneumonia. An area of amorphous calcification (arrow) is seen in the consolidative mass on pre-enhanced mediastinal window CT.

THIN-WALLED CAVITATION

Cavitation in lung cancer is not uncommon and occurs in 2%–16% of cases (7). Typically, the cavity in a malignant tumor has an irregular and uneven thick wall. Nodular extension of tumor (mural nodules) projecting into the lumen of the cavity is frequently seen. Occasionally, cavitating lung cancer may have a smooth and thin wall that can be difficult to be distinguished from benign diseases including a lung abscess and tuberculosis (Fig. 9). Necrotic lung cancer may not develop a bronchial communication and, in that case, which may appear as a fluid-filled mass. Rarely, an air-crescent or meniscus sign can be seen in association with cavitating lung cancer (7, 24).

Lung cancers are often associated with bullae (Fig. 10). Previous studies reported less than 5% of lung cancers arising from bullae (25-27). Lung cancer associated with the bullous disease may have a poor prognosis because the chance of curative surgery can be delayed. Wall thickening of incidentally found a large bulla is often seen probably resulting from inflammatory reactions of the adjacent lung tissue. Therefore, a proper early diagnosis of lung cancer originating from the bulla wall can be difficult on CXR and chest CT is advisable when some changes on CXR are recognized during the follow-up. A malignancy can show irregularity or septation(s) with uneven thickness and accompanying mural nodule(s) on the bulla wall, while a benignancy has a relatively thin and even wall thickness, a smooth inner surface and a homogenous opacity on CT scan.

A unique solitary cystic lung cancer (a thin-walled cystic air-space with a wall thickness of 4 mm or less) also can be a potential cause of the diagnostic error (28). Solitary cystic lung cancer can show nonuniform or nodular cyst wall, septation(s) within the cyst, ground-glass opacities around the cyst, irregular margin, and gradual expansion of the cystic air-spaces (Fig. 11) (28). If the patient has no clinical evidence of inflammation or if there is no improvement of radiologic findings with anti-inflammatory therapy, neoplastic growth should be considered.

AIR-SPACE FILLING PATTERN

Invasive mucinous adenocarcinoma (prior bronchioloalveolar form) can present as an alveolar pattern with an air-space filling process on CXR. This occurs because the tumor may grow

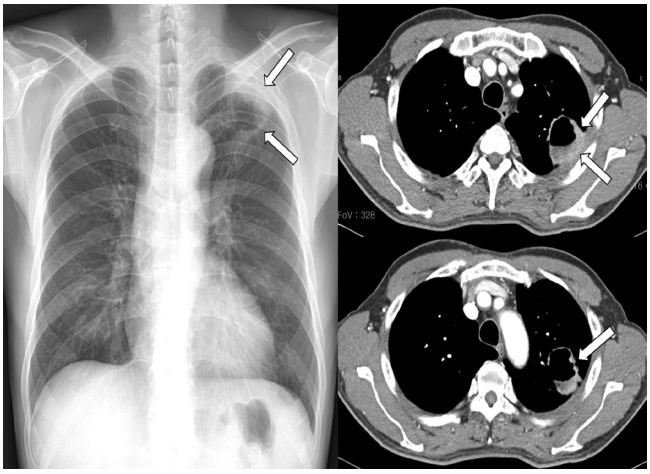

Fig. 9. A 57-year-old man with a squamous cell carcinoma.
There is a cavitating mass with an air-fluid level (arrows) in the periphery of the left upper lobe on chest radiograph, which can be interpreted as a lung abscess or tuberculosis. Contrast-enhanced chest CT shows a mass in the apex of the left lung with necrosis and large cavitation and relatively thin medial wall. However, the uneven thickening of the lateral cavity wall (arrows in upper image) and enhancing mural nodules projecting into the lumen (arrow in lower image) suggest malignancy.

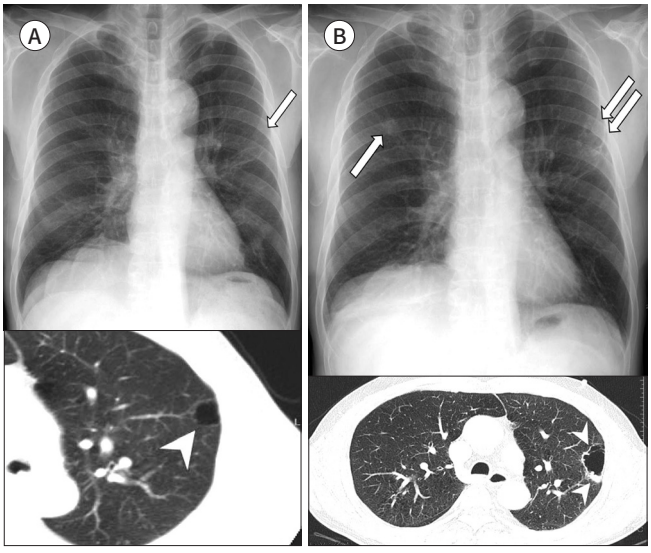

Fig. 10. A 70-year-old man with a squamous cell carcinoma arising from the wall of a bulla.
A. A thin-walled subpleural bulla is retrospectively identified in the left upper lobe on the initial CXR (arrow) and CT (arrowhead).
B. At the 3-year follow-up, enlargement of the subpleural bulla is noted with irregular wall thickening, mural nodules, and septation on CXR (double arrows) and CT (arrowheads). A newly appeared nodule is also seen in the right upper lobe (arrow), which is regarded as a secondary tumor.
CXR = chest radiograph

and spread within the lumen of the distal air-spaces, using the existing stroma of the peripheral lung tissue as its support (7). It can be seen as a focal segmental or nonsegmental consolidation (Fig. 8), a lobar consolidation, or a diffuse air-space filling process that may involve both lungs extensively (Fig. 12). Air-bronchograms are commonly seen (7). It was reported that lung adenocarcinoma mimicking organizing pneumonia can show slow growth and radiologic diagnosis based on the findings of chest CT can be valuable to avoid diagnostic delay (29).

The differential points between the malignancy of air-space filling pattern and pneumonia include clinical findings, the lack of response or progression despite antibiotic treatment or recurrent disease in the same lobe. Also, the presence of associated central mass ("Golden S or reversed S sign") or irregular bronchial narrowing or obstruction, stretching or squeezing of the air-bronchograms within the consolidation can help to make a differential diagnosis of lung cancer (7, 30).

CENTRAL ENDOBRONCHIAL ABNORMALITIES

A delayed diagnosis of central endobronchial diseases commonly occurs because the find-

Fig. 11. A 68-year-old man with a solitary cystic squamous cell carcinoma.
A. A thin-walled large cyst (arrows) in the left upper lobe and left pleural effusion are seen on the initial CXR.
B. Approximately 5 months later, the large cyst in the left upper lobe shows expansion, wall thickening, air-fluid level, and peripheral increased opacity (arrow), which can be interpreted as an infected lung cyst with pneumonia on CXR. Coronal contrast-enhanced chest CT shows mild irregularity in the wall of the solitary cystic lung cancer (arrow) and direct tumor invasion with bone destruction of the thoracic spine (arrowheads). Loculated left pleural effusion with rounded atelectasis is also seen in the left lower lobe.
CXR = chest radiograph

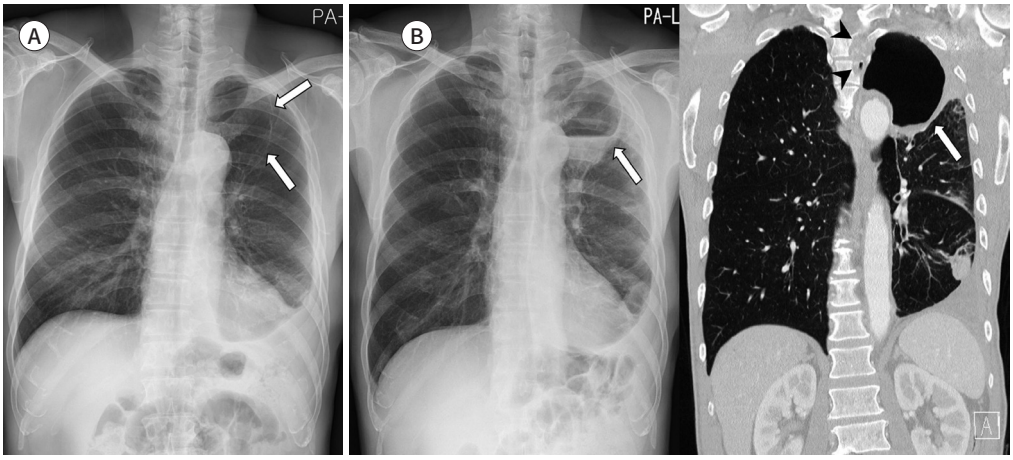

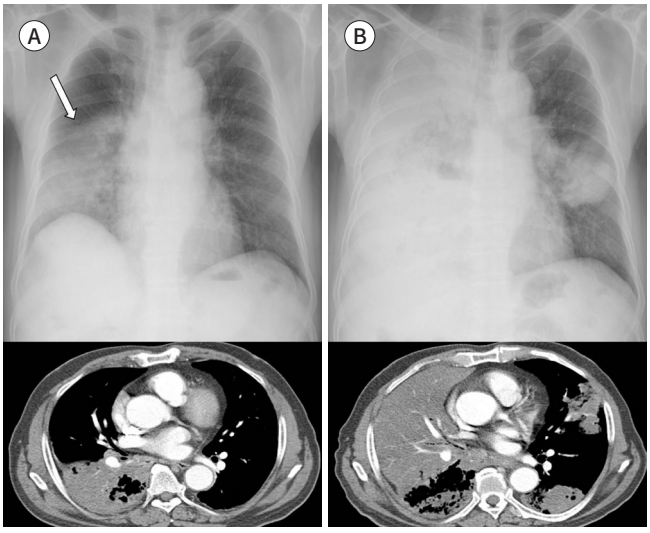

Fig. 12. An 82-year-old man with an invasive mucinous adenocarcinoma and lung to lung metastasis.
A. The initial chest radiograph and CT show an almost lobar air-space consolidation in the right lower lobe (arrow), which can be interpreted as pneumonia.
B. Approximately 4 months later, there is an increased extent of the air-space consolidation in the right lung and a newly appeared lung to lung metastasis with multiple air-space consolidations in the left lung.

ing on CXR is often inconspicuous and is difficult to detect. A CXR may demonstrate almost normal finding or diffuse air-trapping due to partial bronchial obstruction (Fig. 13) or subtle bronchial wall thickening and luminal narrowing in the early stage of diseases (31).

Long continuous bronchial wall thickening is usually caused by inflammatory diseases including infection such as tuberculous or non-tuberculous mycobacterial disease, mucormycosis, aspergillosis and inflammatory diseases such as amyloidosis and sarcoidosis (32). On the other hand, Song et al. (32) reported five cases of primary central squamous cell carcinoma of the lung, which presented as localized and long continuous bronchial thickening (over 2 cm in length) on CT, simulating infectious or inflammatory diseases. This

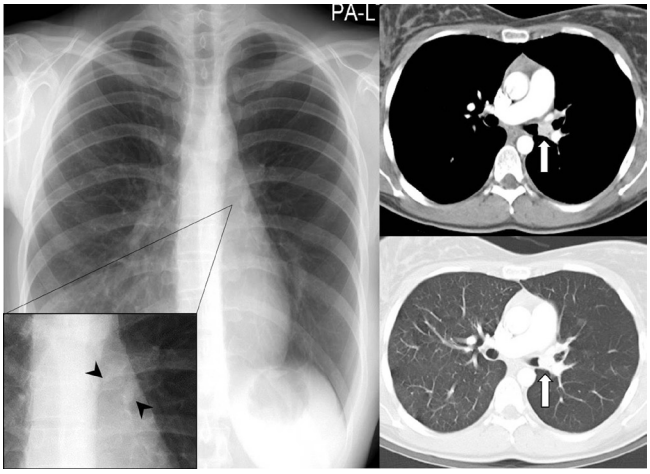

Fig. 13. A 27-year-old woman with a carcinoid tumor. A subtle central endobronchial nodule is seen in the left distal main bronchus on chest radiograph in the magnification view (× 1.4, arrowheads). The diffuse unilateral hyperlucency in the left lung is because of post-obstructive air-trapping. Axial chest CT reveals a well-enhancing endobronchial nodule (arrows) in the left distal main bronchus and diffuse air-trapping in the left lung.

Fig. 14. A 51-year-old woman with an adenoid cystic carcinoma.
A. Abrupt luminal obliteration of the left central airway (arrow) is seen on chest radiograph, which is associated with atelectasis of the left lingular division and left lower lobe and ipsilateral mediastinal shifting. Axial contrast-enhanced chest CT shows diffuse continuous and circumferential wall thickening with luminal narrowing of the left central bronchi and left hilar lymphadenopathy.
B. Bronchoscopy reveals endobronchial protruding masses with hypervascularity.

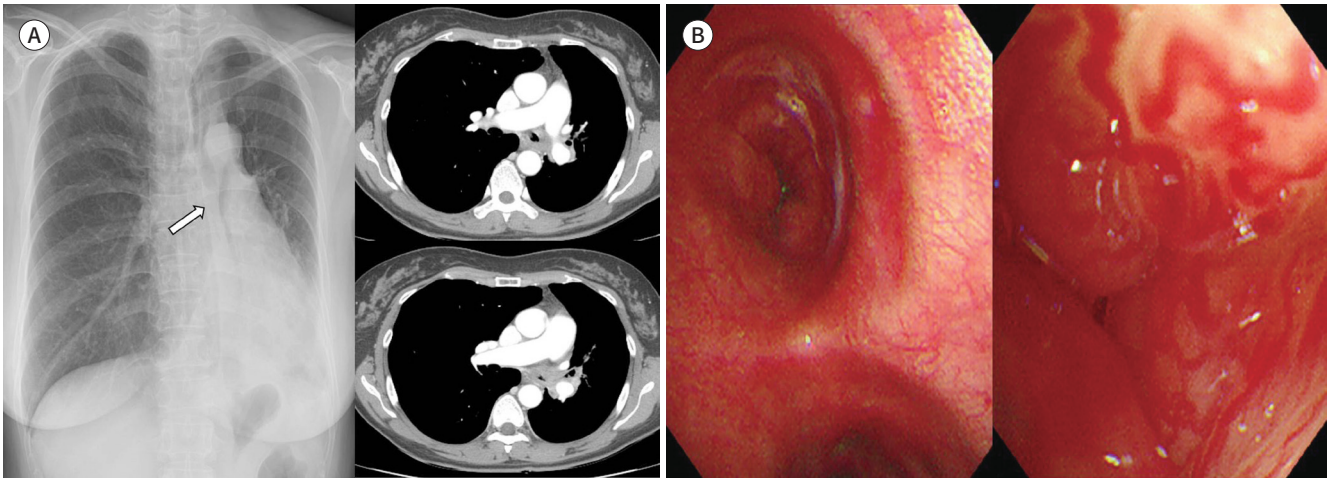

pattern of central squamous cell carcinomas must be very rare, as was reported in only 0.6% and the diagnosis may be delayed due to the similarity with benign diseases. The early manifestation of a bronchogenic carcinoma confined to the bronchial wall can be seen as superficially spreading tumor with slow growth rate and with a greater propensity for longitudinal growth within the mucosa rather than deep tissue invasion. Thus, the differential diagnosis of malignant and benign bronchial wall thickening on CT can be confusing; nevertheless, malignant bronchial wall thickening is to be localized, long, continuous and also bulbous bronchial wall thickening with endobronchial or peribronchial nodule (Fig. 14), whereas benign diseases usually show multifocal, diffuse, or discontinuous bronchial thickening. Malignant bronchial wall thickening may accompany peribronchial lymph node metastasis with adjacent organ invasion or distant metastasis. In benign bronchial wall thickenings such as mycobacterial disease, centrilobular nodules, tree-in-bud

Fig. 15. A 65-year-old man with an adenocarcinoma and coexisting pulmonary TB.
A. Conglomerated calcified nodules with focal pleural thickening are seen in the apex of the right lung on the initial CXR, which are the findings of pulmonary TB.
B. Five months later, pulmonary TB shows no change, and a nodule (arrow) is noted in the right upper lobe overlapping with the right 2nd costochondral junction, which can be retrospectively identified in the corresponding area on the initial CXR (not indicated).
C. Approximately 11 months later, enlargement of a mass in the right upper lobe (arrow) is seen on CXR.
CXR = chest radiograph, TB = tuberculosis

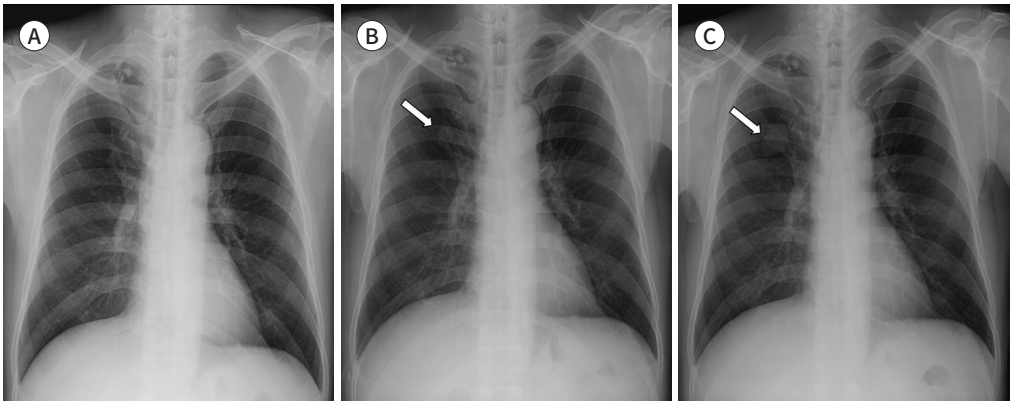

pattern, and cavitary or noncavitary lung nodule can be frequently seen (32-34).

MULTIPLE COEXISTING DISEASES

Another potential observer error can be related to "satisfaction of search," which means "loss of interest" by radiologists after identifying an abnormality. The phenomenon may consequently interfere the search process and the diagnosis of other abnormalities (5). This is related to two possible mechanisms; ceasing the search for other significant abnormalities early in a positive exam and focusing on the "wrong" part of the exam (5). Keep comparison with multiple previous radiographs is an important strategy for reducing missed malignancy (Fig. 15).

CONCLUSION

Missed lung cancer on initial CXR could delay diagnosis and affect the patient's prognosis. Radiologists need to have an effective and efficient search pattern. Every inch of CXR needs to be assessed, and radiologic common blind spots deserve extra attention. Radiologists must develop and train for a routine when examining CXR which ensures that all areas are scrutinized. Awareness of various radiologic presentations of lung cancer and understanding of potential diagnostic pitfalls related to multiple coexisting diseases can contribute to reducing the important diagnostic errors in lung cancer.

A chest radiograph still remains one of the most basic and widely used imaging examinations in radiology. A number of computer-aided diagnosis techniques, such as temporal subtraction augmented by artificial intelligence algorithms, have been developed and successfully applied to many radiologic modalities including CXR. They have demonstrated their utility in the lesion detection and also the diagnosis (35, 36). In this era, radiologists should be better positioned with extensive knowledge and expertise in image interpretation. In particular, the importance of understanding the basics and methods of accurate chest radiographic interpreta-

tion cannot be overemphasized.

Author Contributions

Conceptualization, C.G., N.B.D., H.J.H.; data curation, all authors; formal analysis, C.G., N.B.D., H.J.H.; investigation, all authors; methodology, C.G., N.B.D., H.J.H.; project administration, H.J.H.; resources, all authors; supervision, H.J.H.; validation, H.J.H., K.K., K.H.J., K.D.W.; visualization, C.G., N.B.D., H.J.H.; writing—original draft, C.G., N.B.D., H.J.H.; and writing—review & editing, all authors.

Conflicts of Interest

The authors have no potential conflicts of interest to disclose.

REFERENCES

1. Gibbs JM, Chandrasekhar CA, Ferguson EC, Oldham SA. Lines and stripes: where did they go?--From conventional radiography to CT. *Radiographics* 2007;27:33-48
2. Ellis SM, Flower C. *The WHO manual of diagnostic imaging: radiographic anatomy and interpretation of the chest and the pulmonary system*. Geneva: World Health Organization 2006
3. Quekel LG, Kessels AG, Goei R, Van Engelshoven JM. Miss rate of lung cancer on the chest radiograph in clinical practice. *Chest* 1999;115:720-724
4. Turkington PM, Kennan N, Greenstone MA. Misinterpretation of the chest x ray as a factor in the delayed diagnosis of lung cancer. *Postgrade Med J* 2002;78:158-160
5. Del Ciello A, Franchi P, Contegiacomo A, Cicchetti G, Bonomo L, Larici AR. Missed lung cancer: when, where, and why? *Diagn Interv Radiol* 2017;23:118-126
6. Kashiwabara K, Koshi S, Ota K, Tanaka M, Toyonaga M. Outcome in patients with lung cancer found retrospectively to have had evidence of disease on past lung cancer mass screening roentgenograms. *Lung Cancer* 2002;35:237-241
7. Woodring J. Pitfalls in the radiologic diagnosis of lung cancer. *AJR Am J Roentgenol* 1990;154:1165-1175
8. Qin C, Yao D, Shi Y, Song Z. Computer-aided detection in chest radiography based on artificial intelligence: a survey. *Biomed Eng Online* 2018;17:113
9. Lakhani P, Sundaram B. Deep learning at chest radiography: automated classification of pulmonary tuberculosis by using convolutional neural networks. *Radiology* 2017;284:574-582
10. Hwang EJ, Park S, Jin KN, Kim JI, Choi SY, Lee JH, et al. Development and validation of a deep learning–based automated detection algorithm for major thoracic diseases on chest radiographs. *JAMA Netw Open* 2019;2:e191095
11. Shah PK, Austin JH, White CS, Patel P, Haramati LB, Pearson GD, et al. Missed non–small cell lung cancer: radiographic findings of potentially resectable lesions evident only in retrospect. *Radiology* 2003;226:235-241
12. McLoud TC, Isler RJ, Novelline RA, Putman CE, Simeone J, Stark P. The apical cap. *AJR Am J Roentgenol* 1981;137:299-306
13. Panagopoulos N, Leivaditis V, Koletsis E, Prokakis C, Alexopoulos P, Baltayiannis N, et al. Pancoast tumors: characteristics and preoperative assessment. *J Thorac Dis* 2014;6 Suppl 1:S108-115
14. Monnier-Cholley L, Arrivé L, Porcel A, Shehata K, Dahan H, Urban T, et al. Characteristics of missed lung cancer on chest radiographs: a French experience. *Eur Radiol* 2001;11:597-605
15. De Groot PM, Carter BW, Abbott GF, Wu CC. Pitfalls in chest radiographic interpretation: blind spots. *Semin Roentgenol* 2015;50:197-209
16. Muhm JR, Miller WE, Fontana RS, Sanderson DR, Uhlenhopp MA. Lung cancer detected during a screening program using four-month chest radiographs. *Radiology* 1983;148:609-615
17. Humphrey KL, Wu CC, Gilman MD, El-Sherief AH, Shepard JA, Abbott GF. Where are they all hiding? Common blind spots on chest radiography. *Contemp Diagn Radiol* 2011;34:1-5
18. Sarkar S, Jash D, Maji A, Patra A. Approach to unequal hilum on chest X-ray. *J Assoc Chest Physicians* 2013;1:32
19. Collins J, Stern EJ. *Chest radiology: the essentials*. Philadelphia: Lippincott Williams & Wilkins 2012:1-15
20. Wu CC, Khorashadi L, Abbott GF, Shepard JA. Common blind spots on chest CT: where are they all hiding?

Part 2, Extrapulmonary structures. *AJR Am J Roentgenol* 2013;201:W671-W677
21. Mahoney MC, Shipley RT, Corcoran HL, Dickson BA. CT demonstration of calcification in carcinoma of the lung. *AJR Am J Roentgenol* 1990;154:255-258
22. Fraser RG, Paré JP. *Diagnosis of diseases of the chest*. Philadelphia: W.B. Saunders Company 1978
23. Khan AN, Al-Jahdali HH, Allen CM, Irion KL, Al Ghanem S, Koteyar SS. The calcified lung nodule: what does it mean? *Ann Thorac Med* 2010;5:67-79
24. Hebert C, George RB. Large fluid-filled thoracic mass in a young man. *South Med J* 1988;81:1322-1323
25. Venuta F, Rendina EA, Pescarmona EO, De Giacomo T, Vizza D, Flaishman I, et al. Occult lung cancer in patients with bullous emphysema. *Thorax* 1997;52:289-290
26. Hanaoka N, Tanaka F, Otake Y, Yanagihara K, Nakagawa T, Kawano Y, et al. Primary lung carcinoma arising from emphysematous bullae. *Lung Cancer* 2002;38:185-191
27. Tsutsui M, Araki Y, Shirakusa T, Inutsuka S. Characteristic radiographic features of pulmonary carcinoma associated with large bulla. *Ann Thorac Surg* 1988;46:679-683
28. Tan Y, Gao J, Wu C, Zhao S, Yu J, Zhu R, et al. CT characteristics and pathologic basis of solitary cystic lung cancer. *Radiology* 2019;291:495-501
29. Ichikawa T, Hattori A, Suzuki K, Matsunaga T, Takamochi K, Oh S, et al. Clinicopathological characteristics of lung cancer mimicking organizing pneumonia on computed tomography-a novel radiological entity of pulmonary malignancy. *Jpn J Clin Oncol* 2016;46:681-686
30. Aquino SL, Chiles C, Halford P. Distinction of consolidative bronchioloalveolar carcinoma from pneumonia: do CT criteria work? *AJR Am J Roentgenol* 1998;171:359-363
31. Stevic R, Milenkovic B. Tracheobronchial tumors. *J Thorac Dis* 2016;8:3401-3413
32. Song Y, Choi YW, Paik SS, Han DH, Lee KY. Endobronchial squamous cell carcinoma presenting as localized, long, continuous bronchial thickening on CT. *Eur J Radiol* 2017;91:99-105
33. Traill ZC, Maskell GF, Gleeson FV. High-resolution CT findings of pulmonary sarcoidosis. *AJR Am J Roentgenol* 1997;168:1557-1560
34. Moon WK, Im JG, Yeon KM, Han MC. Tuberculosis of the central airways: CT findings of active and fibrotic disease. *AJR Am J Roentgenol* 1997;169:649-653
35. Shiraishi J, Li Q, Appelbaum D, Doi K. Computer-aided diagnosis and artificial intelligence in clinical imaging. *Semin Nucl Med* 2011;41:449-462
36. Mayo RC, Leung J. Artificial intelligence and deep learning—Radiology's next frontier? *Clin Imaging* 2018;49:87-88

놓치기 쉬운 폐암: 흉부 X선 진단의 함정에 대한 이해와 다양한 폐암 영상 소견의 중요성

최고운[1] · 남보다[1] · 황정화[1*] · 김기업[2] · 김현조[3] · 김동원[4]

흉부 X선은 폐와 종격동 질환을 평가하는 데 있어 매우 중요한 일차 영상 검사이다. 초기 흉부 X선에서 놓친 폐암은 환자의 진단을 지연시키고 예후에 중요한 영향을 줄 수 있다. 저자들은 초기 흉부 X선에서 폐암의 중요한 진단적 오류를 피하기 위하여 비교적 흔히 접하게 되는 영상 진단의 함정에 대하여 다양한 증례를 통하여 검토하고 또한 폐암의 다양한 영상 소견의 중요성에 대하여 중점적으로 살펴보고자 한다.

순천향대학교병원 [1]영상의학과, [2]호흡기알레르기내과, [3]흉부외과, [4]병리과